Grid Synchronization of Power Converters using Multiple Second Order Generalized Integrators

P. Rodríguez[⋆], A. Luna[⋆], I. Candela[⋆], R. Teodorescu[★], and F. Blaabjerg[★]

[⋆]Department of Electrical Engineering
Technical University of Catalonia
Barcelona – SPAIN
prodriguez@ee.upc.edu

[★]Institute of Energy Technology
Aalborg University
Aalborg – DENMARK
ret@iet.aau.dk

***Abstract*-This paper presents a new frequency-adaptive synchronization method for grid-connected power converters which allows estimating not only the positive- and negative-sequence components of the power signal at the fundamental frequency, but also other sequence components at higher frequencies. The proposed system is called the MSOGI-FLL since it is based on a decoupled network consisting of multiple second order generalized integrators (MSOGI) which are frequency-adaptive by using a frequency-locked loop (FLL). In this paper, the MSOGI-FLL is analyzed and its performance is evaluated by both simulations and experiments.**

I. INTRODUCTION

The electricity networks of the future will make an extensive use of power electronics systems and ICT applications. In this sense, the grid-connected power converters applied in distributed power generation systems should be carefully designed and controlled to achieve even better performances than the conventional power plants they replace. One of the most important issues in the connection of power converters to the grid is the synchronization with the grid voltage waveforms. Grid-connected converters should be properly synchronized with the grid to stay actively connected, supporting the grid services (voltage/frequency) and keeping generation up even in the case when the voltages at its point of coupling to the grid are distorted and unbalanced.

In three-phase systems, the PLL based on a synchronous reference frame (SRF-PLL) [1] has become a conventional grid synchronization technique. However, the response of the SRF-PLL is unacceptably deficient when the utility voltage is unbalanced. The decoupled double synchronous reference frame PLL (DDSRF-PLL) [2] overcomes this drawback by using two synchronous reference frames and a decoupling network to insolate the effects of the positive- and negative-sequence voltage components. Another interesting synchronization technique was presented in [3], where three single-phase enhanced phase-locked loops (EPLL) are combined with a positive-sequence calculator to synchronize with unbalanced and polluted three-phase networks without using any synchronous reference frame. A similar approach, but using frequency-locking instead the conventional phase-locking, was presented in [4].

A more precise characterization of the power signals is necessary in those applications in which harmonics components should be selectively controlled. A rigorous analysis of the performance of three real-time algorithms for real-time decomposition of power signals in multiple synchronous reference frames (MSRF) was presented in [5]. Another interesting review of harmonic detection methods was presented in [6]. A detection technique based on using adaptive notch filters for estimating multiple frequencies in a single-phase system is presented in [7].

This paper proposes a new technique for detecting multiple frequency harmonics, with positive- and negative-sequences, in three-phase systems. The proposed system has been named as the MSOGI-FLL since it is based on multiple SOGIs working together inside of a decoupling detection network which is frequency-adaptive thanks to the usage of a FLL.

In the following, the main building blocks of the MSOGI-FLL are presented and the performance of the proposed system is evaluated by both simulations and experiments.

II. THE SECOND ORDER GENERALIZED INTEGRATOR

The concept of the generalized integrator (GI) for sinusoidal signals was formally introduced in [8], where a simplified block with transfer function $2s/(s^2+\omega^2)$ was presented as a GI for single sinusoidal signals. The GI is the base of proportional-resonant (PR) controllers [9]. The basic functionality of the PR controller is to introduce an infinite gain at a selected resonance frequency for eliminating steady state error at that frequency. The GI is also applied to adaptive filtering and PLL implementation [10]. Fig. 1 shows an adaptive filter based on a GI, where as in [10], a cosine function is used to implement the GI, that is:

$$GI(s)=\frac{v'}{k\varepsilon_v}(s)=\frac{s}{s^2+\omega'^2}. \qquad (1)$$

In (1), the resonance frequency was called as ω' to difference it from the input frequency ω. The two in-quadrature output signals of the filter of Fig. 1 are defined by the following

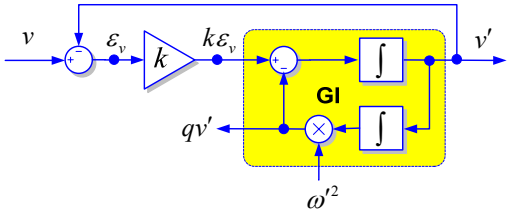

Fig. 1. Adaptive filter based on a GI

978-1-4244-1766-7/08/$25.00 ©2008 IEEE

transfer functions:

$$D(s) = \frac{v'}{v}(s) = \frac{ks}{s^2 + ks + \omega'^2}, \quad (2a)$$

$$Q(s) = \frac{qv'}{v}(s) = \frac{k\omega'}{s^2 + ks + \omega'^2}. \quad (2b)$$

Transfer functions of (2) are not the most suitable choice for implementing a frequency-variable adaptive filter, since both the bandwidth of (2a) and the static gain of (2b) are not only a function of the gain k, but they also depend on center frequency of the filter, ω', which indeed matches the resonance frequency of the GI. To overcome this drawback, an alternative GI structure, named the second order generalized integrator (SOGI) to difference it from the original one, was formally presented in [11]. The adaptive filter based on the SOGI is shown in Fig. 2.

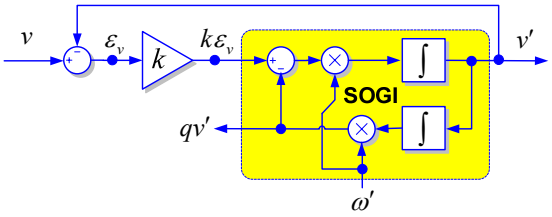

Fig. 2. Adaptive filter based on a SOGI, the SOGI-QSG.

The SOGI transfer function is given by:

$$SOGI(s) = \frac{v'}{k\varepsilon_v}(s) = \frac{\omega' s}{s^2 + \omega'^2}, \quad (3)$$

and transfer functions of the two in-quadrature outputs of the adaptive filter are:

$$D(s) = \frac{v'}{v}(s) = \frac{k\omega' s}{s^2 + k\omega' s + \omega'^2} \quad (4a)$$

$$Q(s) = \frac{qv'}{v}(s) = \frac{k\omega'^2}{s^2 + k\omega' s + \omega'^2} \quad (4b)$$

In this case, the bandwidth of the band-pass filter depicted by (4a) is independent of the center frequency ω', being exclusively set by the gain k. Moreover, transfer functions of (4) evidences that the qv' output is always 90-degrees lagged from the v' output; independently of both the frequency of the v input signal and the resonance frequency of the SOGI. Therefore, the adaptive filter of Fig. 2 was named as SOGI quadrature signal generator (SOGI-QSG)

III. THE FREQUENCY-LOCKED LOOP

The two output signals of the SOGI-QSG have the same amplitude just in the case when the frequency of the input signal and the resonance frequency of the SOGI are equal. Therefore, the center frequency of the SOGI-QSG should be adapted to the frequency of the input signal in order to achieve a balanced set of in-quadrature signals with equal amplitudes at its output.

The frequency-locked loop (FLL) was presented in [4] as an effective mechanism for adapting the center frequency of the SOGI-QSG. The adaptive filter including the FLL is shown in Fig. 3. The relationship between the in-quadrature output signal qv' and the error signal ε_v should be analyzed to explain the behavior of the FLL. The transfer function from the input signal v to the error signal ε_v is given by:

$$E(s) = \frac{\varepsilon_v}{v}(s) = \frac{s^2 + \omega'^2}{s^2 + k\omega' s + \omega'^2}. \quad (5)$$

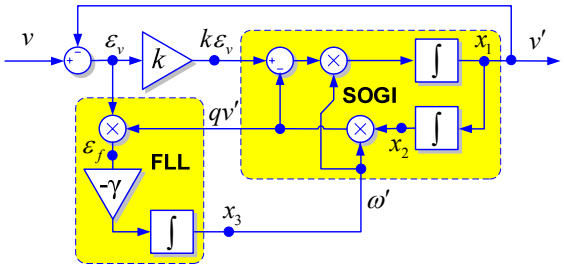

Fig. 3. The SOGI-FLL, a single-phase grid synchronization system.

Both $Q(s)$ and $E(s)$ are plotted together in the Bode diagram of Fig. 4. It can be observed in Fig. 4 that signals qv' and ε_v are in phase when input frequency is lower than the SOGI resonance frequency ($\omega<\omega'$) and they are in counter-phase when $\omega>\omega'$. Therefore, a frequency error variable ε_f can be defined as the product of qv' by ε_v. As indicated in the Bode diagram of Fig. 4, the average value of ε_f will be positive when $\omega<\omega'$, zero when $\omega=\omega'$ and negative when $\omega>\omega'$. Hence, as shown in Fig. 3, an integral controller with a negative gain $-\gamma$, can be used to make zero the dc component of ε_f by shifting the SOGI resonance frequency ω' until matching the input frequency ω. Since the building blocks of the frequency adaptive system of Fig. 3 are the SOGI and the FLL, it was named as the SOGI-FLL, a single-phase synchronization system in which the input frequency is directly detected by the FLL.

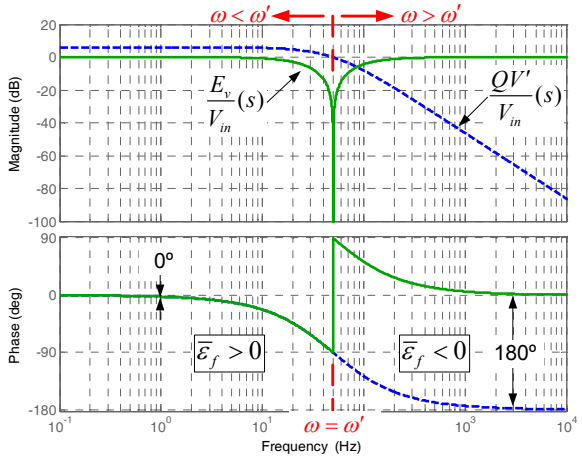

Fig. 4. Bode diagram of the FLL input variables.

IV. ANALYSIS OF THE SOGI-FLL

A. State-space equations

The space-state equations of (6) can be obtained from the system of Fig. 3, being **x** in (6a) the state vector of the SOGI

and **y** in (6b) the output vector. The state equation describing the behavior of the FLL is shown in (6c).

$$\dot{\mathbf{x}} = \begin{bmatrix} \dot{x}_1 \\ \dot{x}_2 \end{bmatrix} = \mathbf{A}\mathbf{x} + \mathbf{B}v = \begin{bmatrix} -k\omega' & -\omega'^2 \\ 1 & 0 \end{bmatrix} \begin{bmatrix} x_1 \\ x_2 \end{bmatrix} + \begin{bmatrix} k\omega' \\ 0 \end{bmatrix} v, \quad (6a)$$

$$\mathbf{y} = \begin{bmatrix} v' \\ qv' \end{bmatrix} = \mathbf{C}\mathbf{x} = \begin{bmatrix} 1 & 0 \\ 0 & \omega' \end{bmatrix} \begin{bmatrix} x_1 \\ x_2 \end{bmatrix}, \quad (6b)$$

$$\dot{\omega}' = -\gamma x_2 \omega' \left(v - x_1\right). \quad (6c)$$

Considering stable operating conditions with $\dot{\omega}' = 0$ and $\omega = \omega'$, (6a) gives rise to (7), in which the steady-state variables are written with a bar over.

$$\dot{\bar{\mathbf{x}}}\Big|_{\dot{\bar{\omega}}'=0} = \begin{bmatrix} \dot{\bar{x}}_1 \\ \dot{\bar{x}}_2 \end{bmatrix} = \begin{bmatrix} 0 & -\omega'^2 \\ 1 & 0 \end{bmatrix} \begin{bmatrix} \bar{x}_1 \\ \bar{x}_2 \end{bmatrix} \quad (7)$$

The eigenvalues of the Jacobian obtained from (7) have a null real part, remaining the steady state response in a periodic orbit at the ω' frequency. Therefore, for a given sinusoidal input signal $v = V\sin\left(\omega t + \phi\right)$ the steady state output vector will be given by:

$$\bar{\mathbf{y}} = \begin{bmatrix} v' \\ qv' \end{bmatrix} = V \begin{bmatrix} \sin\left(\omega t + \phi\right) \\ -\cos\left(\omega t + \phi\right) \end{bmatrix} \quad (8)$$

If the FLL was intentionally 'frozen' at a frequency different from the input signal frequency ($\omega \neq \omega'$), e.g. by making γ=0, the output vector would still keep in a stable orbit defined by:

$$\bar{\mathbf{y}}' = V\left|D(j\omega)\right| \begin{bmatrix} \sin\left(\omega t + \phi + \angle D(j\omega)\right) \\ -\dfrac{\omega'}{\omega}\cos\left(\omega t + \phi + \angle D(j\omega)\right) \end{bmatrix}, \text{ where} \quad (9)$$

$$\left|D(j\omega)\right| = \frac{k\omega\omega'}{\sqrt{\left(k\omega\omega'\right)^2 + \left(\omega^2 - \omega'^2\right)^2}} \text{ and} \quad (10a)$$

$$\angle D(j\omega) = \arctan\frac{\omega'^2 - \omega^2}{k\omega\omega'}. \quad (10b)$$

B. Local stability

It is possible to appreciate from (9) that the SOGI states keep the following steady-state relationship when a sinusoidal input signal at the frequency ω is applied to its input:

$$\dot{\bar{x}}_1 = -\omega^2 \bar{x}_2. \quad (11)$$

Therefore, the steady-state synchronization error signal can be written from (6a) as:

$$\bar{\varepsilon}_v = \left(v - \bar{x}_1\right) = \frac{1}{k\omega'}\left(\dot{\bar{x}}_1 + \omega'^2 \bar{x}_2\right). \quad (12)$$

From (11) and (12), the steady-state frequency error signal is given by:

$$\bar{\varepsilon}_f = \omega' \bar{x}_2 \bar{\varepsilon}_v = \frac{\bar{x}_2^{\,2}}{k}\left(\omega'^2 - \omega^2\right). \quad (13)$$

Expression (13) corroborates that the signal ε_f collect information about error in frequency estimation and hence it is suitable to act as the control signal of the FLL. An analysis about local stability of the FLL can be conducted by considering $\omega' \approx \omega$. In such case, $\omega'^2 - \omega^2$ can be approximated as $2\left(\omega' - \omega\right)\omega'$, and the local dynamics of the FLL can be described by:

$$\dot{\omega}' = -\gamma\bar{\varepsilon}_f = \frac{\gamma}{k}\bar{x}_2^{\,2}\left(\omega'^2 - \omega^2\right) \approx -2\frac{\gamma}{k}\bar{x}_2^2\left(\omega' - \omega\right)\omega' \quad (14)$$

Defining the error in frequency estimation as σ=(ω'-ω), its derivative is given by $\dot{\sigma} = \dot{\omega}'$ (ω is considered a constant). Therefore, the condition of (15) will be always true for positive values in the detected frequency ω'. This condition is the key for the local stabilization mechanism of the FLL.

$$\sigma\dot{\sigma} = -2\frac{\gamma}{k}\bar{x}_2^2\sigma^2\omega' \leq 0 \quad (15)$$

C. SOGI-QSG tuning

From the transfer functions of (4), the time response of the SOGI-QSG for a given sinusoidal input signal $v = V\sin\left(\omega t + \phi\right)$ is described by:

$$v' = -\frac{V}{\lambda}\sin\left(\lambda\omega t\right)\cdot e^{-\frac{k\omega'}{2}t} + V\sin\left(\omega t\right), \quad (16a)$$

$$qv' = V\left[\cos\left(\lambda\omega t\right) + \frac{k}{2\lambda}\cdot\sin\left(\lambda\omega t\right)\right]e^{-\frac{k\omega'}{2}t} - V\cos\left(\omega t\right), \quad (16b)$$

where $\lambda = \sqrt{4 - k^2}/2$ and k<2.

According to (16), the settle time in the SOGI-QSG response can be approximated to:

$$t_{s(SOGI)} = \frac{10}{k\omega'}. \quad (17)$$

In this work, the gain of the SOGI-QSG is set to $k = \sqrt{2}$, which results in an optimal trade off between settle time, overshooting and harmonics rejection.

D. FLL tuning

Taking a sinusoidal signal $v = V\sin\left(\omega t + \phi\right)$ as input signal for the SOGI-FLL and considering an unstable FLL operating point with $\omega' \neq \omega$, the square of the state $\bar{x}_2$ can be written from (9) as:

$$\bar{x}_2^2 = \frac{V^2}{2\omega^2}\left|D(j\omega)\right|^2\left[1 + \cos\left(2\left(\omega t + \phi + \angle D(j\omega)\right)\right)\right]. \quad (18)$$

In the vicinity of the steady-state operation of the FLL, the nonlinear term of the dynamics equation (14), $\bar{x}_2^2$, will present a dc component equal to $V^2/2\omega^2$ plus an ac term oscillating at twice the input frequency. Therefore, the averaged dynamics of the FLL with $\omega' \approx \omega$ can be described by (19), where the ac component of $\bar{x}_2^2$ has been neglected.

$$\dot{\bar{\omega}}' = -\frac{\gamma V^2}{k\omega'}\left(\bar{\omega}' - \omega\right) \quad (19)$$

Equation (19) is very interesting because it discloses the relationship between the dynamic response of the FLL and the grid variables and SOGI-QSG gain. From (19), the value of γ can be normalized according (20) in order to obtain the

linearized system of Fig. 5, which is nondependent on neither the grid variables nor the SOGI-QSG gain.

$$\gamma = \frac{k\omega'}{V^2}\Gamma \tag{20}$$

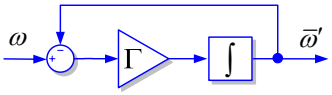

Fig. 5. Simplified frequency adaptation system of the FLL.

The transfer function of the first-order frequency adaptation loop of Fig. 5 is given by:

$$\frac{\bar{\omega}'}{\omega} = \frac{\Gamma}{s+\Gamma}. \tag{21}$$

Therefore, the settle time is exclusively dependent on the design parameter Γ and can be approximated by:

$$t_{s(FLL)} \approx \frac{5}{\Gamma}. \tag{22}$$

The feedback-based linearized FLL is shown in Fig. 6. In this system, the FLL gain is adjusted in runtime by feeding-back the estimated grid operating conditions, which guarantees constant settle time in grid frequency estimation independently of input signal characteristics.

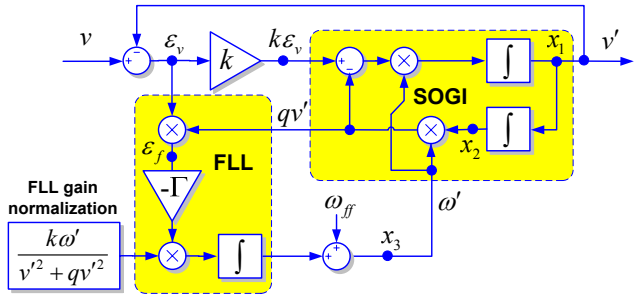

Fig. 6. SOGI-FLL with FLL gain normalization.

Fig. 7 shows the time response of a SOGI-FLL with $k=\sqrt{2}$ and $\Gamma=50$ when the frequency of the input signal suddenly varies from 50 Hz to 45 Hz. The detected frequency fits well a first-order exponential response with a settle time of 100 ms, which matches to that calculated by (22).

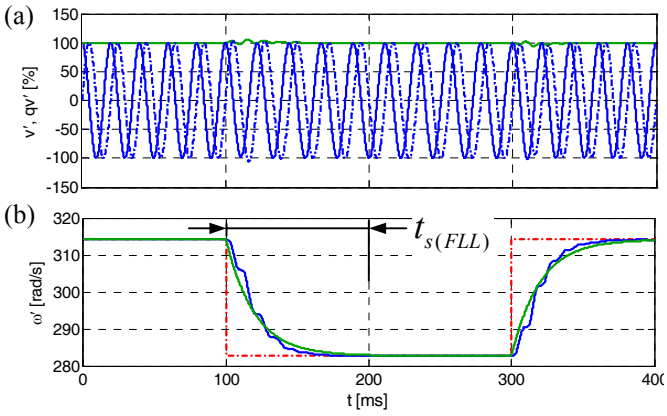

Fig. 7. Time response of the FLL in presence of a frequency step.

V. THE MSOGI-FLL APPLIED TO DISTORTED GRIDS

The low-order harmonics close to the fundamental frequency give rise to remarkable distortion levels on the signals detected by the DSOGI-FLL. In this section, a cross-feedback network consisting of multiple SOGI-QSGs tuned at different frequencies is presented as an effective solution to accurately detect the sequence components of the grid voltage even under very extreme distortion conditions. This new detection system is shown in Fig. 8 and it will be referred from now on as the Multiple SOGI-FLL (MSOGI-FLL).

The MSOGI-FLL of Fig. 8 consists of *n* individual SOGI-QSGs working in a collaborative way by using a cross-feedback network. Each of these SOGI-QSGs is tuned to a different frequency multiple of the fundamental frequency. The FLL inputs are provided by the SOGI-QSG-1, which is tuned at the fundamental frequency. The tuning frequency fro the rest of SOGI-QSGs (from 2 to *n*) is set by multiplying the fundamental frequency detected by the FLL by a coefficient which determines the order of the harmonic assigned to each SOGI-QSG. Moreover, the gain of each SOGI-QSG is divided by the order such coefficient in order to maintain a constant relationship between center frequency and the bandwidth of the SOGI-QSG. The MSOGI-FLL presents an interesting feature resulting from the usage of a cross-feedback network. As shown in Fig. 8, the input signal of each SOGI-QSG is calculated by subtracting the output of all the rest of SOGI-QSGs from the original input signal *v*. In this way, after a transient process, the input signal of each SOGI-QSG is cleaned up from the harmonic components detected by the rest of SOGI-QSGs, which will reduce the

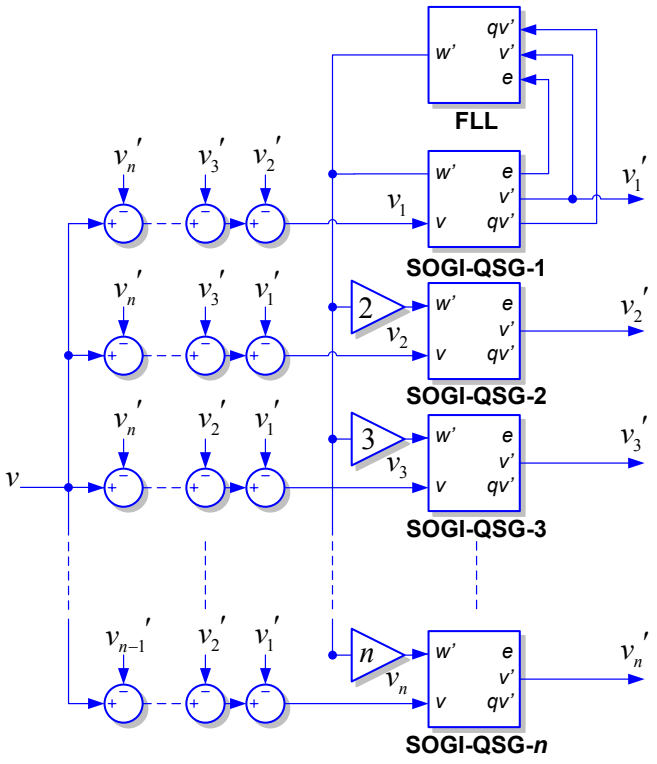

Fig. 8. Block diagram of the MSOGI-FLL.

distortion at its output. Therefore, the output of the i^{th} SOGI-QSG in a MSOGI-FLL structure with n elements is given by:

$$v_i' = D_i(s)\left(v - \sum_{\substack{j=1 \\ j\neq i}}^{n} v_j'\right), \tag{23}$$

where $D_i(s)$ is a customized version of the transfer function of (4a) in which the center frequency is now given by $i\cdot\omega'$; being ω' the fundamental frequency detected by the FLL.

By developing the equations system resulting from (23), the next transfer function is obtained for the i^{th} SOGI-QSG:

$$v_i' = \left[D_i(s)\prod_{\substack{j=1 \\ j\neq i}}^{n}\left(\frac{1-D_j(s)}{1-D_i(s)D_j(s)}\right)\right]v \ . \tag{24}$$

Fig. 9 shows the Bode diagram for the transfer function of (24) for a MSOGI-FLL consisting of four individual SOGI-QSGs tuned at the 2nd, 4th, 5th and 7th harmonics. The dashed line in Fig. 9 represents the frequency response curve for the case in which the cross-feedback network is deactivated. This diagram shows how the cross-feedback network gives rise to notches in the frequency response curve at the frequencies which the individual SOGI-QSG are tuned to. As a consequence, the selective filtering characteristic of each SOGI-QSG is improved and the overall response is enhanced in case of high distortion level on the input voltage.

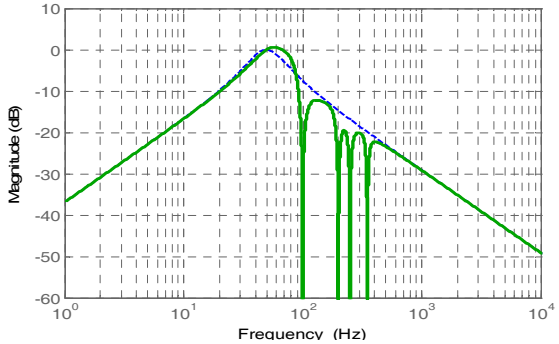

Fig. 9. Frequency response of the single-phase MSOGI-FLL.

A three-phase MSOGI-FLL can be easily implemented by applying the single-phase structure of Fig. 8 to the two orthogonal signals of the $\alpha\beta$ stationary reference frame. As was shown [4], the output of these dual SOGIs working on the $\alpha\beta$ domain (DSOGI) will provide the input signals to a positive-/negative-sequence calculator which is in charge of calculating the instantaneous positive- and negative-sequence symmetrical components at the tuning frequency of the correspondent DSOGI. According to §III, each SOGI-QSG of a DSOGI-FLL would have an independent FLL. Although mathematically correct, the use of several independent FLLs might however seem conceptually odd since the frequencies of both v_α and v_β signals of the DSOGI are always identical. For this reason, this work proposes the usage of a single FLL combining the frequency error signals from both α and β axes. The gain of such a FLL is normalized by using the square of the amplitude of the positive-sequence component at the fundamental frequency, $(v_\alpha^{+1})^2 + (v_\beta^{+1})^2$.

VI. Simulation Results

An unbalanced and highly distorted grid voltage was considered for demonstrating by simulation the excellent performance of a three-pahse MSOGI-FLL. During the grid fault, the positive- and negative-sequence voltage phasors at the fundamental frequency were set to $\vec{V}^{+1} = 0.5\angle -30º$ and $\vec{V}^{-1} = 0.25\angle 110º$ –with a pre-fault grid voltage given by $\vec{V}_{pf} = 1\angle 0º$. Regarding harmonics, they were set to $\vec{V}^{-5} = 0.2\angle 0º$, $\vec{V}^{+7} = 0.2\angle 0º$ and $\vec{V}^{-11} = 0.2\angle 0º$ for the 5th, 7th and 11th harmonics, respectively. Moreover, to set a harder scenario, a step on the fundamental frequency from 50 Hz to 45 Hz occurred during the simulated grid fault.

The MSOGI-FLL considered in this simulation consisted of four individual DSOGIs tuned at the 1st, 5th, 7th and 11th harmonics. The gain for the DSOGI tuned at the fundamental frequency was set to $k_1 = \sqrt{2}$. The gain for the rest of DSOGIs was divided by the harmonic order. The dc gain of the FLL was set to $\Gamma = 50$.

Fig. 10(a) shows the unbalanced and distorted grid voltage applied to the input of the MSOGI-FLL. Figs. 11(b) and 11(c) show how the detection of the positive- and negative-sequence components is practically perfect in spite of the high pollution level existing on the grid voltage and the sudden step on the grid frequency. Finally, Fig. 10(d) shows the evolution of the detected fundamental grid frequency. It is possible to appreciate in this figure how the feedback-based linearization of the FLL works well even under hard distorted conditions, matching the settle time to that calculated by (22).

VII. Experimental Results

To experimentally validate the performance of the synchronization system presented in this paper, the algorithm of the MSOGI-FLL was implemented in a control board based on the floating point DSP Texas Instruments TMS320F28335 at 150 MHz. The sampling frequency was set to 10 kHz. The unbalanced and distorted input voltage was generated by an AC programmable source ELGAR SM5250A. The parameters of the unbalanced and distorted input voltage are described in Table I.

The MSOGI-FLL was implemented with seven embedded DSOGIs (one per each harmonic plus the fundamental one).

TABLE I
Parameters of the Input Voltage

Voltage component	Value [p.u.]
Fundamental frequency positive-sequence	$\vec{V}^{+1} = 0.733\angle 5º$
Fundamental frequency negative-sequence	$\vec{V}^{+1} = 0.210\angle 50.4º$
2nd harmonic negative-sequence	$\vec{V}^{-2} = 0.10\angle 0º$
3rd harmonic zero-sequence	$\vec{V}^{03} = 0.10\angle 45º$
4th harmonic positive-sequence	$\vec{V}^{+4} = 0.10\angle 180º$
5th harmonic negative-sequence	$\vec{V}^{-5} = 0.25\angle 45º$
7th harmonic positive-sequence	$\vec{V}^{+7} = 0.20\angle 180º$
11th harmonic negative-sequence	$\vec{V}^{-11} = 0.15\angle 180º$

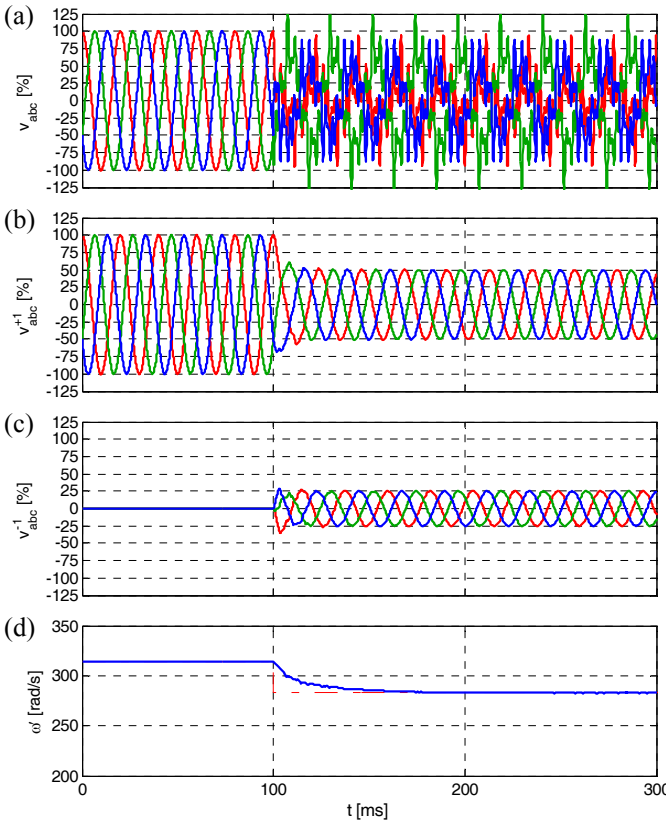

Fig. 10. Response of the MSOGI-FLL.

Fig. 11 shows some scopes recorded from the experimental plant. Fig. 11(a) shows the input voltage, which was unbalanced and extremely distorted. Figs. 11(b) and 11(c) show the waveforms detected for the positive- and negative-sequence components at the fundamental frequency. According to the results shown in this scopes, it is worth to point out the excellent performance of the MSOGI-FLL what, in addition to its low computational burden, makes the synchronization system proposed in this paper very suitable to be applied in real-time controllers of power converters connected to the grid.

VIII. CONCLUSIONS

A new concept in grid-synchronization of power converters under unbalanced and distorted operating conditions, the MSOGI-FLL, has been introduced in this paper. The MSOGI-FLL consists of multiple DSOGIs (SOGI-QSGs in the case of single-phase systems) tuned at different harmonics of the fundamental grid frequency (from 1 to *n*). These DSOGIs work in a collaborative way by using a cross-feedback network, which allows decoupling the effect of the different harmonics of the input voltage on the input signals of each DSOGI. The MSOGI-FLL only uses one FLL, which is connected to the DSOGI tuned at the fundamental frequency. Simulations together with an experimental evaluation were presented in order to demonstrate that the MSOGI-FLL is a very suitable solution to the detection of fundamental-frequency positive- and negative-sequence components of unbalanced and distorted grid voltages.

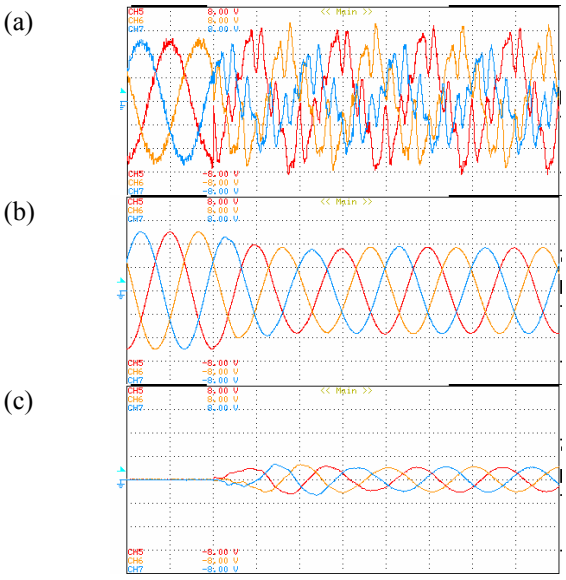

Fig. 11. Experimental response of the MSOGI-FLL.

ACKNOWLEDGMENT

This work was supported by the projects ENE2007-67878-C02-00/ALT, ENE2008-06841-C02-01/ALT and HBP2006-044.

REFERENCES

[1] S. Chung, "A phase tracking system for three phase utility interface inverters," *IEEE Trans. Power Electron.*, vol. 15, pp. 431-438, May 2000.

[2] P. Rodriguez, J. Pou, J. Bergas, J.I. Candela, R.P. Burgos, and D. Boroyevich, "Decoupled Double Synchronous Reference Frame PLL for Power Converters Control," *IEEE Trans. Power Electron.*, vol.22, no.2, pp.584-592, Mar. 2007.

[3] M. Karimi-Ghartemani and M.R. Iravani, "A method for synchronization of power electronic converters in polluted and variable-frequency environments," *IEEE Trans. Power Systems*, vol. 19, pp. 1263-1270, Aug. 2004.

[4] P. Rodriguez, A. Luna, M. Ciobotaru, R. Teodorescu, and F. Blaabjerg, "Advanced Grid Synchronization System for Power Converters under Unbalanced and Distorted Operating Conditions," *in Proc. IEEE Ind. Electron. Conf. (IECON'06)*, Nov. 2006, pp.5173-5178.

[5] V.M. Moreno, M. Liserre, A. Pigazo, A. Dell'Aquila , "A Comparative Analysis of Real-Time Algorithms for Power Signal Decomposition in Multiple Synchronous Reference Frames," *IEEE Trans. Power Electron.*, vol.22, no.4, pp.1280-1289, July 2007.

[6] L. Asiminoaei, F. Blaabjerg, S. Hansen, "Detection is key - Harmonic detection methods for active power filter applications," *IEEE Ind. Applicat. Magazine*, vol.13, no.4, pp.22-33, July-Aug. 2007.

[7] M. Mojiri, M. Karimi-Ghartemani, A. Bakhshai, "Time-Domain Signal Analysis Using Adaptive Notch Filter," *IEEE Transactions on Signal Processing*, vol.55, no.1, pp.85-93, Jan. 2007

[8] Yuan, X., Merk, W., Stemmler, H., and Allmeling, J., "Stationary frame generalized integrators for current control of active power filters with zero steady-state error for current harmonics of concern under unbalanced and distorted operating conditions," *IEEE Trans. Ind. Appl.*, vol. 38, no.2, pp. 523–532, Mar./Apr. 2002.

[9] R. Teodorescu, F. Blaabjerg, M. Liserre, and P.C. Loh, "Proportional-resonant controllers and filters for grid-connected voltage-source converters," *Electric Power Applications, IEE Proceedings*, vol. 153, no.5, pp. 750-762, Sept. 2006.

[10] K. de Brabandere, T. Loix, K. Engelen, B. Bolsens, J. Van den Keybus, J. Driesen, and R. Belmans, "Design and Operation of a Phase-Locked Loop with Kalman Estimator-Based Filter for Single-Phase Applications," *in Proc. IEEE Ind. Electron. Conf. (IECON'06)*, Nov. 2006, pp. 525-530.

[11] P. Rodriguez, R. Teodorescu, I. Candela, A.V. Timbus, M. Liserre, and F. Blaabjerg, "New Positive-sequence Voltage Detector for Grid Synchronization of Power Converters under Faulty Grid Conditions," *in Proc. IEEE Power Electron. Spec. Conf. (PESC'06)*, Jun. 2006, pp. 1-7.